The pterocarpanquinone LQB-118 compound induces apoptosis of cytarabine-resistant acute myeloid leukemia cells

THAÍS HANCIO[1], LUCIANO MAZZOCCOLI[1], GUSTAVO GUIMARÃES[1], MARCELA ROBAINA[1], BRUNA DOS SANTOS MENDONÇA[1], GABRIELA NESTAL DE MORAES[1], BARBARA DA COSTA REIS MONTE-MOR[2], LUCIANA MAYUMI GUTIYAMA[2], LUÍZE OTERO DE CARVALHO[3], CHAQUIP DAHER NETTO[4], PAULO R.R. COSTA[5], FERNANDA COSTAS CASAL DE FARIA[1] and RAQUEL CIUVALSCHI MAIA[1]

[1]Laboratory of Cellular and Molecular Hemato-Oncology, Program of Molecular Hemato-Oncology; [2]Laboratory of Molecular Biology, Bone Marrow Transplant Center (CEMO); [3]Stem Cell Laboratory, Bone Marrow Transplant Center (CEMO), Brazilian National Cancer Institute (INCA), Rio de Janeiro, RJ 20230-130; [4]Chemistry Laboratory, Federal University of Rio de Janeiro (UFRJ), Macaé Campus, Rio de Janeiro, RJ 27930-560; [5]Bioorganic Chemistry Laboratory, Natural Products Research Institute (IPPN), Rio de Janeiro Federal University (UFRJ), Rio de Janeiro, RJ 21941-599, Brazil

Received May 26, 2020; Accepted January 19, 2021

DOI: 10.3892/ijo.2021.5204

Abstract. Acute myeloid leukemia (AML) is a complex hematological disorder characterized by blockage of differentiation and high proliferation rates of myeloid progenitors. Anthracycline and cytarabine-based therapy has remained the standard treatment for AML over the last four decades. Although this treatment strategy has increased survival rates, patients often develop resistance to these drugs. Despite efforts to understand the mechanisms underlying cytarabine resistance, there have been few advances in the field. The present study developed an *in vitro* AML cell line model resistant to cytarabine (HL-60R), and identified chromosomal aberrations by karyotype evaluation and potential molecular mechanisms underlying chemoresistance. Cytarabine decreased cell viability, as determined by MTT assay, and induced cell death and cell cycle arrest in the parental HL-60 cell line, as revealed by Annexin V/propidium iodide (PI) staining and PI DNA incorporation, respectively, whereas no change was observed in the HL-60R cell line. In addition, the HL-60R cell line exhibited a higher tumorigenic capacity *in vivo* compared with the parental cell line. Notably, no reduction in tumor volume was detected in mice treated with cytarabine and inoculated with HL-60R cells. In addition, western blotting revealed that the protein expression levels of Bcl-2, X-linked inhibitor of apoptosis protein (XIAP) and c-Myc were upregulated in HL-60R cells compared with those in HL-60 cells, along with predominant nuclear localization of the p50 and p65 subunits of NF-κB in HL-60R cells. Furthermore, the antitumor effect of LQB-118 pterocarpanquinone was investigated; this compound induced apoptosis, a reduction in cell viability and a decrease in XIAP expression in cytarabine-resistant cells. Taken together, these data indicated that acquired cytarabine resistance in AML was a multifactorial process, involving chromosomal aberrations, and differential expression of apoptosis and cell proliferation signaling pathways. Furthermore, LQB-118 could be a potential alternative therapeutic approach to treat cytarabine-resistant leukemia cells.

Correspondence to: Professor Raquel Ciuvalschi Maia, Laboratory of Cellular and Molecular Hemato-Oncology, Program of Molecular Hemato-Oncology, Brazilian National Cancer Institute (INCA), Praça da Cruz Vermelha, 23, 6º andar., Rio de Janeiro 20230-130, Brazil
E-mail: rcmaia@inca.gov.br

Key words: cytarabine, LQB-118, drug resistance, acute myeloid leukemia

Introduction

Acute myeloid leukemia (AML) is a complex hematological disorder characterized by blockage of differentiation and high proliferation rates of myeloid progenitors, leading to bone marrow (BM) failure (1,2). AML has an incidence of ~20,000 new cases per year in the United States (3) and is associated with very high mortality rates (4,5). AML incidence rates in Brazil vary according to region, mainly due to socioeconomic inequalities that impact healthcare access and appropriate diagnosis. Although Brazilian records do not differentiate the incidence between leukemia types, 5,920 cases in men and 4,890 in women are expected in 2020-2022 for all types of leukemia, and AML is the most common type of leukemia in adults (6). The reduced overall survival (OS) rate of patients with AML is intrinsically related to resistance of leukemia cells to therapy, with the majority of patients initially achieving remission and later progressing to a more aggressive disease (7,8).

The standard therapy for AML, which includes anthracycline and cytarabine, has remained unchanged over the last 40 years; however, it is inefficient at prolonging OS and curing a large majority of patients, except for those with promyelocytic leukemia (9,10). Pyrimidine analogues, such as cytarabine, are the key drugs used to treat AML and present a chemical structure similar to cytosine (11,12). Despite efforts made to understand the mechanisms underlying cytarabine resistance in AML, only a few advances have been made (13,14), this may be because it involves multiple molecular mechanisms (15). Some pathways involved in apoptosis evasion, including increased levels of the inhibitor of apoptosis proteins (IAPs) and imbalanced expression of Bcl-2 family proteins, have been reported to have key roles in cytarabine resistance and poor prognosis (16-19).

Other pathways involved in chemotherapy resistance involve dysregulated expression and function of transcription factors, such as c-Myc and NF-κB (20-22). In addition, c-Myc expression has been associated with BM stromal cell-mediated resistance in AML cell lines, and high c-Myc expression has been associated to high cytogenetic risk and poor prognosis in patients with AML (23,24).

Since most patients develop resistance to AML standard therapy, the search for alternative treatment options is essential. The LQB-118 synthetic compound has been reported to exert antitumoral effects on AML cells with a multidrug resistant (MDR) profile. The LQB-118 compound has also exhibited cytotoxic effects on chronic myeloid leukemia (CML) MDR cell lines and patient samples. Its antitumor activity in AML and CML cells has been associated with reduced expression of survivin and X-linked IAP (XIAP) anti-apoptotic proteins, and modulation of NF-κB subcellular localization (25-29).

The present study developed an *in vitro* AML cell line model resistant to cytarabine and investigated the mechanisms underlying the development of chemoresistance. Moreover, the potential antitumor effect of LQB-118 on a cytarabine-resistant AML cell line was assessed; to the best of our knowledge, this has not been previously investigated. The present study aimed to better understand the mechanisms underlying cytarabine resistance in an AML-resistant cell line and investigated the potential antitumor effect of LQB-118 compound in a cytarabine-resistant cell line.

Materials and methods

Cell culture, generation of a cytarabine-resistant cell line and drug treatment. HL-60 (ATCC® CCL-240™/P53 null; American Type Culture Collection) and HL-60R human cell lines (FAB M2) were cultured in RPMI (Gibco; Thermo Fisher Scientific, Inc.) supplemented with 10% heat-inactivated fetal bovine serum (Gibco; Thermo Fisher Scientific, Inc.) and 2 mM L-glutamine (Sigma-Aldrich; Merck KGaA). The HL-60R cell line was obtained through culturing HL-60 parental cells with increasing doses of cytarabine (Accord Farmacêutica Ltd.). Concentrations ranged between 0.001 and 50 μM, doubling every three passages, for 6 months. The cell lines were maintained in a humidified incubator (Thermo Fisher Scientific, Inc.) at 37˚C and 5% CO_2, and the HL-60R cell line was continuously cultured with 50 μM cytarabine. The drug was withdrawn 24 h prior to subsequent assays. Cell lines were tested for *Mycoplasma* contamination by PCR and the genotypes were confirmed by short tandem repeat. The LQB-118 synthetic compound was developed and produced by Dr Paulo Costa and Dr Chaquip Netto in the Laboratory of Bioorganic Chemistry at the Natural Products Research Institute of the Federal University of Rio de Janeiro (Rio de Janeiro, Brazil) (29). For experiments with the LQB-118 compound, HL-60 and HL-60R cells were incubated with different concentrations of the compound (1.5, 3, 6 and 9 μM for MTT assay; 3 μM for other assays) for 24 h at 37˚C. Untreated cells (cultures in drug-free media) or cells treated with the vehicle dimethyl sulfoxide (DMSO) were used as experimental controls.

Cytotoxicity assay. HL-60 and HL-60R cell viability was evaluated using the MTT assay following treatment with cytarabine, idarubicin (Chemicaltech Farmacêutica), daunorubicin (Farmarin) or with the LQB-118 compound. A total of $2x10^4$ cells/well were seeded in 96-well plates and treated with increasing drug concentrations. After 24, 48 and 72 h, cells were incubated with the MTT reagent (Sigma-Aldrich; Merck KGaA) in a humidified incubator at 37˚C and 5% CO_2 for 4 h. Formazan crystals were then solubilized in DMSO and the absorbance was measured at 570 nm using a spectrophotometer (EZ Read 400; Biochrom Ltd.).

Cell cycle progression and cell death detection. For assessment of cell cycle progression and cell death following treatment with cytarabine or LQB-118, cells were incubated with 50 μM cytarabine for 48 h or 3 μM LQB-118 for 24 h. Subsequently, $2x10^5$ cells were centrifuged (750 x g at room temperature for 3 min), washed with PBS (pH 7.4) and incubated with Annexin V, Alexa Fluor™ 488 conjugate (cat. no. A13201; Invitrogen; Thermo Fisher Scientific, Inc.) for 15 min at room temperature. Subsequently, propidium iodide (PI) was added to the cells and cell death index was evaluated by assessing the Annexin V/PI-marked cells by flow cytometry. In order to evaluate the total apoptosis rate induced by the compounds, early (Annexin V^+/PI^-) and late (Annexin V^+/PI^+) apoptosis was considered. Cell cycle progression was evaluated by PI DNA incorporation. After treatment with cytarabine or LQB-118 compound, $3x10^5$ cells were centrifuged (750 x g at room temperature for 3 min), washed with PBS, and incubated with 100 μg/ml RNAse (100 μg/ml ribonuclease A diluted in 40 mM citrate buffer; Sigma-Aldrich; Merck KGaA) and 50 μg/ml PI (50 μg/ml diluted in 40 mM citrate buffer with 0.3% Triton X-100) for 15 min at room temperature. Finally, cells were analyzed in a flow cytometer. Cells in both assays were assessed using the CyAn ADP analyzer flow cytometer and Summit v4.3 software was used for analysis (both from Beckman Coulter, Inc.). Three independent experiments were performed.

Karyotype evaluation. For karyotyping, cells were initially cultured in a concentration of $1x10^7$ cells/ml for 24 h. A total of 2 h before the end of this incubation, cells were treated with colchicine (0.05 μg/ml) and maintained in a humidified incubator at 37˚C and 5% CO_2 for 1 h. Subsequently, cells were incubated with hypotonic solution (0.075 M KCl) for 15 min for chromosome preparation, followed by a fixation step with

Carnoi solution (3:1, methanol:acetic acid) for 20 min at room temperature. To obtain GTG banding patterns, the slides were incubated for 10-14 sec at room temperature in 0.1% trypsin solution in Dulbecco's solution [0.137 M NaCl, 0.0027 M KCl, 0.0015 M KH_2PO_4, 0.011 M NaH_2PO_4 (pH 6.8)], washed with saline solution (0.9% NaCl) and stained with 2% Giemsa (Merck KgaA) solution in phosphate buffer for 15 min at room temperature. Chromosomes were identified and classified according to the International System of Nomenclature of Human Cytogenetics 2016 (30) and chromosomal analysis was performed under optical microscopy using at least 30 metaphases per cell line. The images were acquired through the Cytovision Applied Image Karyotyping System (Leica Microsystems, Inc.) for at least 5 to 10 metaphases for the assembly of karyotypes.

Analysis of FLT3 internal tandem duplications (ITDs), and CEBPA, DNMT3A, IDH1, IDH2 and NPM1 gene mutations. DNA was extracted from $1x10^7$ HL-60 and HL-60R cells using the automated Maxwell® system (Promega Corporation). Genomic regions of interest were amplified by PCR using specific primers for *CEBPA*, *DNMT3A* exon 23, *IDH1* exon 4 and *IDH2* exon 4. For amplification of targeted regions in *CEBPA*, PCR was performed using 1 unit Platinum™ Taq DNA Polymerase High Fidelity, 1X PCR buffer, 2 mM $MgSO_4$, 400 μM dNTPs (all from Thermo Fisher Scientific, Inc.), 1 M betaine, 400 nM each primer (Integrated DNA Technologies, Inc.) and 0.1 μg DNA. The thermal profile for amplification was: 94˚C for 5 min; 34 cycles [94˚C for 30 sec; 65˚C for 30 sec; 68˚C for 1 min]; 68˚C for 10 min. For amplification of targeted regions in DNMT3A and IDH1/2, the PCR reactions were performed using Taq polymerase (1 unit for DNMT3A or 2.5 units for IDH1/2), 1X PCR buffer, 1.5 mM $MgCl_2$, 250 μM dNTPs (all from Thermo Fisher Scientific, Inc.), 400 nM each primer (Integrated DNA Technologies, Inc.) and 0.1 μg DNA. The thermal profile for amplification was: 94˚C for 3 min; 35 cycles (94˚C for 30 sec; 60˚C for 30 sec; 72˚C for 1 min); 72˚C for 10 min. Primer sequences are provided in Table SI. After purification with PureLink PCR purification kit (Invitrogen; Thermo Fisher Scientific, Inc.), amplicons were submitted to direct sequencing with BigDye Terminator v3.1 Cycle Sequencing kit (Thermo Fisher Scientific, Inc.) on an ABI 3130xl Genetic Analyzer (Applied Biosystems; Thermo Fisher Scientific, Inc.). Sequence data files were analyzed using Mutation Surveyor software V4.0.9 (SoftGenetics, LLC).

For *FLT3* and *NPM1* gene expression analysis, RNA was isolated from $5x10^6$ cells using TRIzol® reagent (Invitrogen; Thermo Fisher Scientific, Inc.). For cDNA synthesis, reverse transcription (RT) was performed using 200 units ImProm II Reverse transcriptase, 1X RT buffer, 3 mM $MgCl_2$ (all from Promega Corporation), 0.2 μg random primers, 500 μM dNTPs, 40 units RNaseOUT (all from Thermo Fisher Scientific, Inc.) and 2 μg RNA. RNA was initially incubated at 65˚C, for 5 min, and RT was performed at 42˚C for 40 min and stopped at 65˚C for 5 min. *FLT3* ITDs or *NPM1* mutations were screened by PCR using specific fluorescent primers. For amplification of targeted regions in *FLT3* and *NMP1*, the PCR reactions were performed using 1.5 units Taq Platinum polymerase, 1X PCR buffer, 2.0 mM $MgCl_2$, 200 μM dNTPs (all from Thermo Fisher Scientific, Inc.), 400 nM each primer (Integrated DNA Technologies, Inc.) and 2 μl cDNA. The thermal profile for amplification was: 94˚C for 5 min; 30 cycles (94˚C for 30 sec; 56˚C for 45 sec; 72˚C for 30 sec); 72˚C for 20 min, followed by fragment analysis on ABI 3130xl Genetic Analyzer (Applied Biosystems; Thermo Fisher Scientific, Inc.). Sequences were analyzed using Chimer Marker software V3.0.2 (SoftGenetics, LLC).

RT-quantitative PCR (RT-qPCR). HL-60 and HL-60R total RNA was extracted with TRIzol reagent according to the manufacturer's instructions. For RT-qPCR, RNA was reverse transcribed into cDNA using SuperScript II Reverse Transcriptase (Invitrogen; Thermo Fisher Scientific, Inc.) according to the manufacturer's protocol. Subsequently, qPCR (TaqMan® Gene Expression Assay; Applied Biosystems; Thermo Fisher Scientific, Inc.) was performed using the following Taqman probes (Applied Biosystems; Thermo Fisher Scientific, Inc.): *MYC* (Hs00153408_m1) and *β-actin* (NM_001101.2). Thermocycling conditions were as follows: Incubation at 50˚C for 2 min and 95˚C for 10 min, followed by 40 denaturation cycles at 95˚C for 15 sec, and annealing and extension at 60˚C for 1 min in the StepOne™ System (Applied Biosystems; Thermo Fisher Scientific, Inc.). *β-actin* was used as an endogenous reference gene. The $2^{-\Delta\Delta Cq}$ method was used to calculate relative expression (31).

Western blotting and cell fractionation. Whole cell lysates were obtained using protein Cell Extraction Buffer (Invitrogen; Thermo Fisher Scientific, Inc.) and nuclear/cytoplasm fractionation was performed with the NE-PER™ Nuclear and Cytoplasmic Extraction Reagents kit (Thermo Fischer Scientific, Inc.), according to the manufacturers' instructions. Protein content was measured using the DC™ Protein Assay (Bio-Rad Laboratories, Inc.) according to manufacturer's instructions. Total proteins (20-30 μg) were separated by SDS-PAGE on 10 or 12% gels and were transferred to Hybond-P membranes (GE Healthcare). Prior to antibody incubation, membranes were blocked with 5% nonfat milk for 1 h at room temperature. All primary antibodies were incubated overnight (16-24 h) at 4˚C and secondary antibodies were incubated for 1 h at room temperature. After all antibody incubations, membranes were washed with Tris-buffered saline with 0.05% Tween 20 (Sigma-Aldrich; Merck KGaA). Anti-Bcl-2 (1:200 dilution, clone 124; cat. no. IS61430-2; Dako; Agilent Technologies, Inc.), anti-BAK (1:1,000 dilution, polyclonal; cat. no. 3814; Cell Signaling Technology, Inc.), anti-Bax (1:1,000 dilution, SPM 336; cat. no. sc-65532; Santa Cruz Biotechnology, Inc.), anti-XIAP (1:1,000 dilution, 3B6; cat. no. 2045; Cell Signaling Technology, Inc.), anti-c-Myc (1:1,000 dilution, 9E10; cat. no. sc-40; Santa Cruz Biotechnology,), anti-NF-κB1 p105/p50 (1:1,000 dilution, polyclonal; cat. no. 3035; Cell Signaling Technology, Inc.), anti-NF-κB p65 (1:1,000 dilution, C22B4; cat. no. 4764; Cell Signaling Technology, Inc.), anti-cleaved caspase-3 (1:500 dilution, Asp175; 5A1E; cat. no. 9664; Cell Signaling Technology, Inc.), anti-pro-caspase 3 (1:500 dilution, CPP32; cat. no. 610322; BD Biosciences) anti-β-actin (1:1,000 dilution, AC-15; cat.no. A5441; Sigma-Aldrich; Merck KGaA), anti-lamin B (1:1,000 dilution, cat. no. NA12; Calbiochem; Merck KGaA) and anti-Hsc70 (1:1,000 dilution,

B-6; cat. no. sc-7298; Santa Cruz Biotechnology, Inc.) were used as primary antibodies for western blotting. Anti-mouse IgG (1:10,000 dilution; cat. no. A9169; Sigma Aldrich; Merck KGaA) and anti-rabbit IgG-HRP conjugated (1:10,000 dilution; cat. no. A9044; Sigma Aldrich; Merck KGaA) were used as secondary antibodies. The Clarity Max kit (Bio-Rad Laboratories, Inc.) was used to visualize protein expression and blots were detected using the C-digit digital system (LI-COR Biosciences). Analyses were performed using ImageJ software version 1.53E (National Institutes of Health).

Protein phosphorylation profiling. The protein phosphorylation profiles of the HL-60 and HL-60R cell lines were compared using the Human Phospho-Kinase Antibody Array (cat. no. ARY003B; R&D Systems, Inc.), according to manufacturer's instruction.

AML xenograft model. BALB/c-nude mice were purchased from Jackson Laboratory and maintained in specific pathogen-free conditions in the animal facility of the Brazilian National Cancer Institute (INCA) all animal experiments were approved by the Animal Ethics Committees of INCA. For *in vivo* experiments, 34 male BALB/c nude mice (age, 8-12 weeks; n=16 mice/HL-60 group; n=18 mice/HL-60R group) were used. Weight was measured before randomization, and mean weight was 28.33±0.66 kg (presented as mean ± SEM). Mice were housed in microisolator cages, with a maximum of five mice per cage, with sterilized food and water given *ad libitum*, in an air-filtered specific pathogen-free (SPF) area. Mice were kept under a 12-h light/dark cycle, and the SPF area was maintained at 18-23˚C with 40-60% humidity. The *in vivo* growth capacity of the AML cell lines was tested using a subcutaneous xenograft model. To establish this model, $5x10^6$ HL-60 or HL-60R cells were resuspended in 100 μl PBS and injected subcutaneously into the right flank of male BALB/c nude mice (age, 8-12 weeks; n=16 mice/HL-60 group; n=18 mice/HL-60R group). The animals were monitored daily for tumor signal over a 58-day period. After appearance, tumor dimensions were measured every day using a digital caliper, and the tumor volume (mm^3) was calculated using the following formula: $0.52x(d^2xD)$, where d and D refer to the smallest and largest tumor diameters, respectively. The tumorigenesis ratio (%) was evaluated using the following formula: $N^+/Nx100$, where N^+ is the number of mice with tumor presence and N is the number of injected mice (32-35).

To evaluate the response of HL-60R cells to cytarabine *in vivo*, mice were randomized into two experimental groups (vehicle or cytarabine; n=4 mice/group) with the same mean tumor volume (50 mm^3) on day 14 post-injection. Cytarabine (100 mg/kg) and vehicle (water) were then administered every day for 5 days by intraperitoneal injection with a 22G needle (33). The welfare and weight of the mice were monitored daily to assess cytarabine toxicity. On day 15 post-randomization, when the first mouse reached the largest tumor diameter of 20 mm, all mice were anesthetized with 2% isoflurane and images were captured. All mice that presented with a maximum tumor diameter of 20 mm on this day were euthanized by CO_2 asphyxiation (20%/min). Mice that did not reach the maximum tumor diameter (20 mm) on day 15 post-randomization were followed up until they reached the maximum tumor diameter and were then euthanized.

Statistical analyses. Statistical analyses were conducted using GraphPad Prism software (PRISM 5.0; GraphPad Software Inc.). For data analysis, one-way ANOVA followed by Bonferroni post-hoc test was applied to the results of the MTT assay, cell death and DNA fragmentation assays evaluating the effects of the LQB-118 compound. Unpaired Student's t-test was performed to analyze cell death, DNA fragmentation and MTT assays comparing HL-60 and HL-60R cells. In addition, Kaplan-Meier and log-rank test was performed to assess *in vivo* survival. $P<0.05$ was considered to indicate a statistically significant difference.

Results

HL-60R cells demonstrate resistance to cytarabine but not to anthracyclines used in AML treatment. First, the cytarabine-resistant HL-60R cell line was generated by continuously exposing the HL-60 parental cell line to increasing concentrations of this drug. Once the cell line treatment reached 50 μM and the cells continued to proliferate in culture, model validation was performed.

The present study assessed whether cytarabine treatment could induce cell death and inhibit viability of the HL-60 and HL-60R cell lines. The results demonstrated that cytarabine impaired cell viability in the HL-60 cell line in a time-dependent manner, whereas no change was observed in the HL-60R cell line (Fig. 1A-C). Cell viability was significantly reduced in the HL-60 cell line in response to treatment with 2.5 μM cytarabine for 24 h when compared to HL-60R cells in the same condition ($P<0.001$; Fig. 1A). Furthermore HL-60R cells remained viable even when exposed to 200 μM cytarabine for 72 h (Fig. S1). Moreover, treatment with 50 μM cytarabine for 48 h enhanced the percentage of Annexin V^+ cells ($P=0.0180$; Fig. 2A and B) and DNA fragmentation ($P=0.0004$; Figs. 2C and S2B) in the HL-60 cell line, but not in the HL-60R cell line in the same conditions. In HL-60 cells, cell cycle profile analysis indicated cell cycle arrest after cytarabine treatment (Fig. S2a) and high levels of DNA fragmentation were detected at 48 h. After 24 h of cytarabine treatment, more cells in the G_2/M phase were detected in the HL-60 group (data not shown). Anthracyclines are chemotherapeutic agents used alongside cytarabine in AML treatment (36,37). Thus, the present study investigated whether the HL-60R cell line exhibited cross resistance to anthracyclines. Although HL-60 cells were shown to be more sensitive to idarubicin and daunorubicin treatment at earlier time-points, HL-60R cell viability was similarly decreased in a time and dose-dependent manner (Fig. S3A-F). These data indicated that HL-60R cells exhibited resistance to cytarabine but sensitivity to anthracyclines used in AML treatment. Therefore, the HL-60R cell line may be a useful model to understand specific pathways involved in acquisition of cytarabine resistance.

HL-60R cells present a complex karyotype and do not harbor mutations involved in AML development and chemoresistance. Karyotype complexity and mutation profile are predictive and prognostic factors for AML, being related to complete response to induction therapy and OS (36). Therefore, the present study

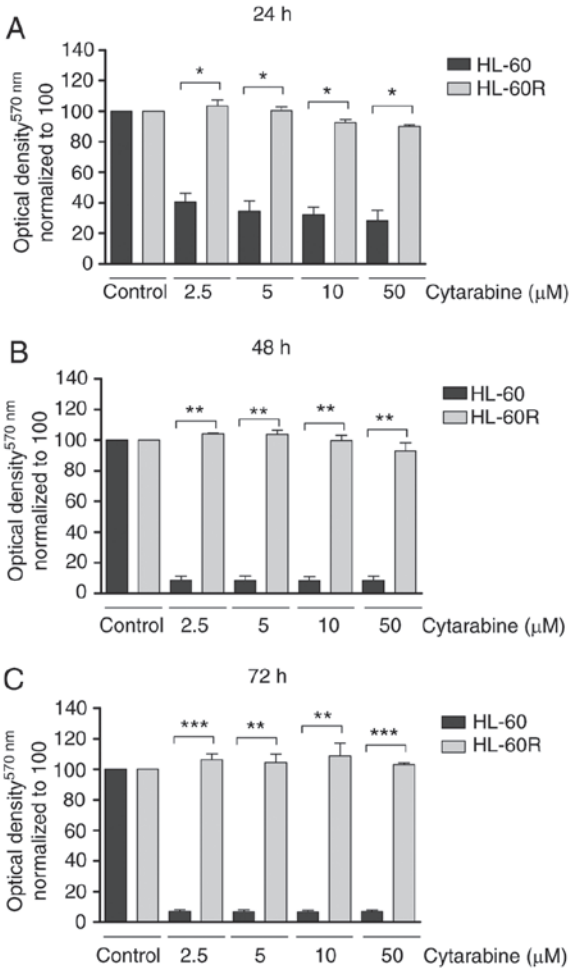

Figure 1. Cytarabine has no effect on cytarabine-resistant cell line viability. HL-60 and HL-60R cells were treated with 2.5-50 μM cytarabine and cell viability was evaluated by MTT assay after (A) 24 h, (B) 48 h and (C) 72 h. Optical density was normalized to the control group, which was set at 100. Data are presented as the mean ± SD of three independent experiments. Statistical significance was determined by Student's t-test. *P≤0.05, **P≤0.01, ***P≤0.001.

investigated the karyotype and mutational profile in HL-60 parental and resistant cell lines. The results demonstrated that both cell lines presented complex karyotypes, based on the presence of three or more chromosomal alterations (Fig. S4). The HL-60 cell line comprised two subpopulations coexisting in the same cell culture, both of which presented 45 chromosomes, with only one X chromosome. One of the subpopulations presented the karyotype: Ins (4q), -5, add (9) (p13), del(10)(p12), add(17)(p13), -18, +2mar, whereas the other possessed the karyotype: Ins (4q), -5, add(9)(p13), del (10) (p12), add (17)(p13), -18, +3mar (Fig. S4). The HL-60R cell line presented only one population, demonstrating a karyotype with 48 chromosomes and the presence of two X chromosomes, -8, -9, + 14, + 15, + 18, + 20, del (9q) (Fig. S4). Subsequently, possible mutations in *CEBPA*, *DNMT3A*, *IDH1*, *IDH2* and *NPM1*, as well as *FLT3* ITDs were investigated. Notably, no mutations in the genes analyzed were detected in either cell line (Fig. S5) further suggesting that these gene alterations may not have a role in the HL-60R resistance model.

HL-60R cells induce increased tumorigenicity in vivo and preserve cytarabine resistance in subcutaneous xenograft models. The present study compared the ability of HL-60 and HL-60R AML cell lines to generate tumors in xenograft models. HL-60 and HL-60R cell lines were inoculated into 16 and 18 mice, respectively. The results demonstrated that the HL-60R cell line presented a higher tumorigenic capacity *in vivo* compared with the HL-60 cell line, HL-60R and HL-60 cells induced tumorigenesis in 44.44 and 18.75% mice, respectively (Table I).

The present study evaluated the response of the HL-60R cell line to cytarabine treatment *in vivo*. Due to the low number of animals with tumors in the HL-60 group, only the HL-60R group was used in this experiment. After 14 days of HL-60R inoculation, mice with tumor growth were randomized into two experimental groups: Vehicle and cytarabine (100 mg/kg as a single dose, intraperitoneal, for 5 days). Notably, no reduction in tumor volume was observed in the cytarabine-treated group when compared with the vehicle group (Fig. 3A and B). An increase in tumor volume of the animals treated with cytarabine (day 15: 1,506±468.6 mm^3) was detected in relation to the vehicle group (day 15: 893.2±576 mm^3), but this increase was not statistically significant. Notably, the treatment protocol exhibited no apparent toxicity, and body weight and welfare were maintained (Fig. S6A). The survival curves showed no difference between the two groups (Fig. S6B), reinforcing the ability of the HL-60R cell line to retain resistance to cytarabine *in vivo*.

Cytarabine resistance is associated with increasing levels of transcription factors, and anti-apoptotic and proliferation-inducing proteins. In order to understand the pathways involved in cytarabine resistance in the HL-60R cell line, the expression levels of proteins involved in apoptosis signaling, which could be differentially expressed, were evaluated. Although similar expression levels of Bax and BAK pro-apoptotic proteins were detected, the HL-60R cell line exhibited upregulation of Bcl-2 and XIAP anti-apoptotic proteins compared with in the HL-60 cell line (Fig. 4A). Furthermore, the expression levels of c-Myc, which is highly associated with proliferation in numerous types of cancer (38), was investigated. HL-60R cells presented higher protein expression levels of c-Myc compared with the parental cell line (Fig. 4A). Notably, there was no difference in c-Myc mRNA expression levels between HL-60 and HL-60R cells (Fig. S7), suggesting that degradation of the c-Myc protein may be reduced in HL-60R cells.

NF-κB expression and localization has been associated with resistance to chemotherapy in certain types of cancer, including AML (20-22). Therefore, the present study investigated the localization and expression of p50 and p65 subunits of NF-κB in the HL-60R cell line. The results demonstrated that the p50 and p65 subunits exhibited enhanced nuclear localization in the HL-60R cell line compared with in the parental cell line (Fig. 4B).

Due to the multifactorial profile associated with cytarabine resistance, a phospho-kinase array was performed to compare the phosphorylation profile of HL-60R cells and the parental cell line, HL-60. Notably, the results demonstrated that HL-60 and HL-60R cells exhibited a different phosphorylation profile, suggesting the involvement of several signaling pathways in cytarabine resistance (Fig. 4C-E). The expression of phosphorylated proteins was increased in both

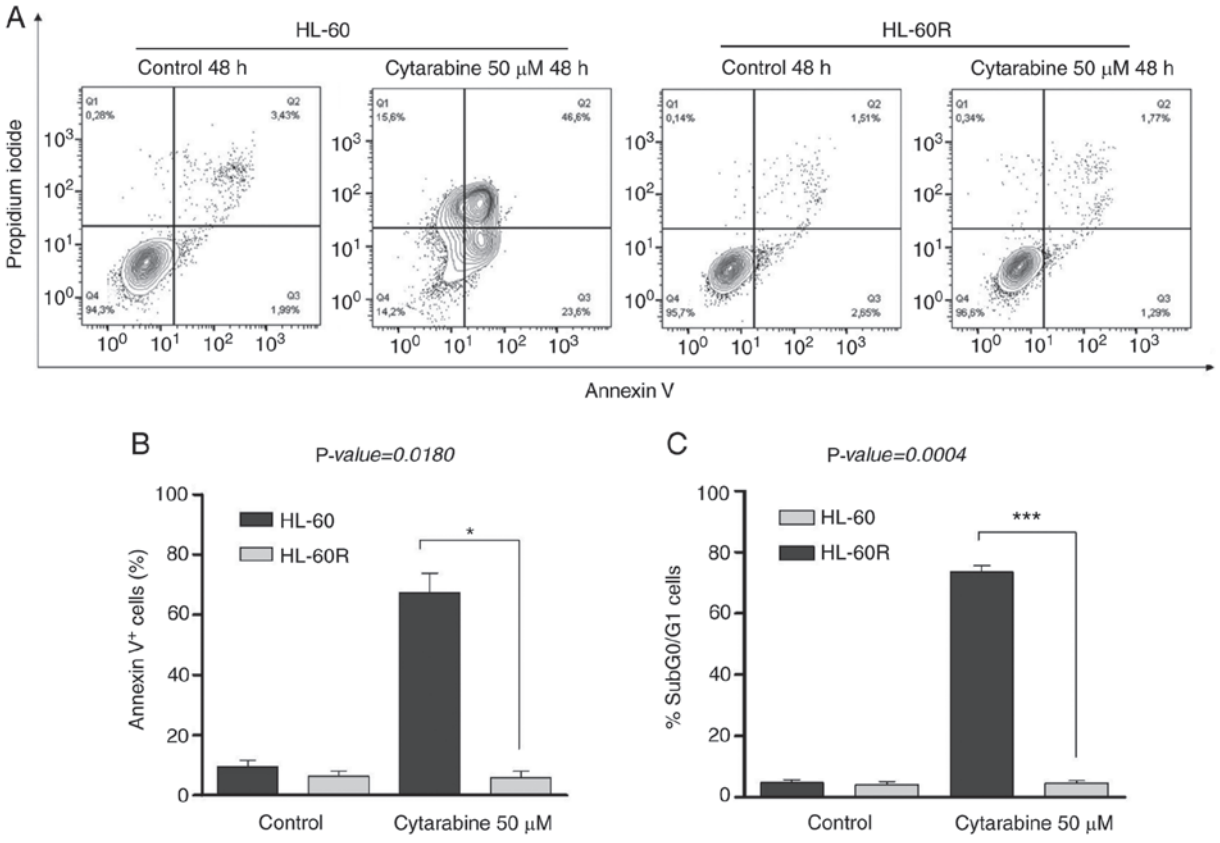

Figure 2. Cytarabine-resistant cells are not affected by cytarabine treatment. HL-60 and HL-60R cells were treated with 50 μM cytarabine for 48 h. After treatment, cell death was evaluated by (A and B) Annexin V$^+$ detection by flow cytometry and (C) DNA fragmentation analysis. Data are presented as the mean ± SD of three independent experiments. Statistical significance was determined by Student's t-test. *P≤0.05, ***P≤0.001.

cytarabine-resistant and -sensitive cells. Notably, the array revealed that AKT oncogenic kinase, which is widely related to proliferation and survival in several tumor types, including AML (39), exhibited reduced phosphorylation in the HL-60R cell line. This result was further validated by western blotting, where the differential expression of phosphorylated-AKT was confirmed in cytarabine-sensitive and cytarabine-resistant cells (Fig. 4F). Taken together, these findings clearly indicated that the acquisition of cytarabine resistance in AML was a complex process, involving the modulation of numerous oncogenic signaling pathways.

LQB-118 exhibits cytotoxicity against cytarabine-resistant cells. Our previous studies demonstrated the cytotoxic activity of the synthetic LQB-118 compound in several types of cancer, including AML (25-29,40-43). Therefore, the present study aimed to investigate the antitumor effect of the LQB-118 compound particularly in cells resistant to cytarabine. Notably, HL-60 and HL-60R cells treated with different concentrations of LQB-118 exhibited a very similar response after 24, 48 and 72 h, as determined by MTT assay (Fig. 5A and B).

In order to investigate the potential of LQB-118 to induce cell death in cytarabine-resistant cells, the HL-60R cell line was treated with 3 μM LQB-118 for 24 h and apoptosis was evaluated by DNA fragmentation analysis, Annexin V staining, and analysis of pro-caspase 3 and cleaved caspase 3 protein expression levels. After treatment, an increase in Annexin V$^+$ cell percentage was detected (P≤0.01; Fig. 6A and B), and pro-caspase-3 expression was reduced and caspase-3 cleavage was increased (Fig. 6C) in HL-60R cells compared with the vehicle group. Furthermore, PI incorporation analysis revealed that 3 μM LQB-118 treatment for 24 h in HL-60R cells increased DNA fragmentation compared with in the vehicle group (P<0.001; Fig. 7A and C), whereas there was no alteration in cell cycle profile (Fig. 7B and D). Taken together, these data demonstrated that LQB-118 treatment induced apoptosis of HL-60R cells, with little effect on cell cycle progression.

The present study investigated the expression levels of Bcl-2 and XIAP anti-apoptotic proteins after LQB-118 treatment, as these proteins were differentially expressed in HL-60R cells compared with in HL-60 cells. The results demonstrated that treatment of HL-60R cells with 3 μM LQB-118 for 24 h did not alter Bcl-2 protein expression levels (Fig. 8A), but it did decrease XIAP protein expression levels (Fig. 8B), suggesting that XIAP may be involved in the mechanism underlying the effects of LQB-118 on the induction of apoptosis of HL-60R cells.

Discussion

The major obstacle for successful treatment of AML, the most common type of acute leukemia in adults, is intrinsic or acquired resistance following the induction of remission treatment (8,44-47). Although some mechanisms have been implicated in cytarabine resistance, there is no clear

Table I. HL-60R cells exhibit increased formation of subcutaneous tumors *in vivo*.

Cell type	Follow-up, days	Number of injected mice	Number of mice with tumor presence	Tumorigenesis ratio, %
HL-60	58	16	3	18.75
HL-60R	58	18	8	44.44

Tumorigenesis ratio was determined according to the following formula: $N^+/Nx100$, where N refers to number of injected mice and N^+ refers to number of mice with tumor presence.

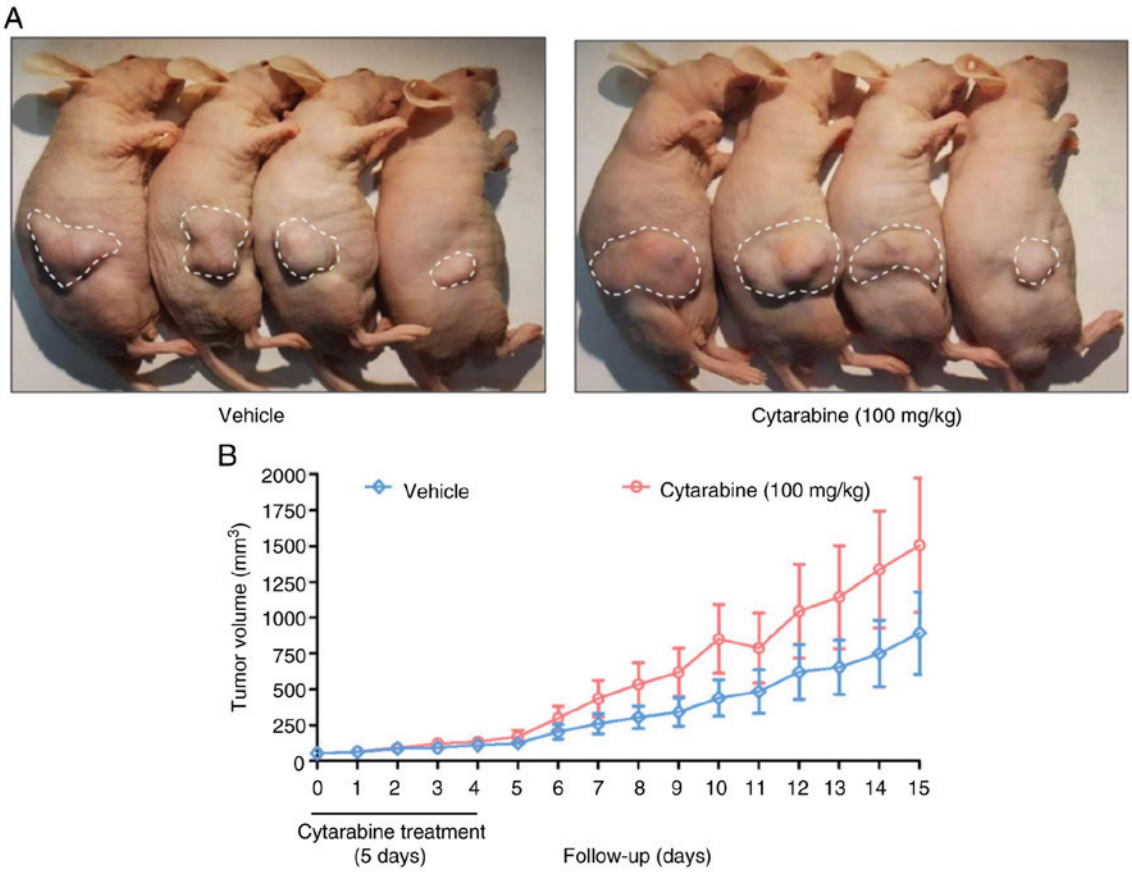

Figure 3. HL-60R cells induce higher tumorigenicity compared with HL-60 cells and do not respond to cytarabine *in vivo*. Mice were randomized and treated intraperitoneally with vehicle or cytarabine (100 mg/kg) for 5 days. The experiment lasted 15 days after onset of treatment. Mice were euthanized when tumor volume reached the limit. (A) Randomized mice in the vehicle and cytarabine (100 mg/kg) experimental groups 15 days after treatment. (B) Tumor volume of experimental groups over 15 days. Data are presented as the mean ± SEM. Statistical significance was determined by Student's t-test.

comprehension of this multifactorial phenomenon. The HL-60R cell line was developed from the HL-60 parental cell line, first described as a promyelocytic/FAB M3 subtype and later as a FAB M2 subtype due to the lack of promyelocytic characteristics, such as t(15;17) (48,49). The HL-60 cell line has been widely used as an *in vitro* model to understand leukemogenesis and treatment response (50). Although some groups have attempted to generate cytarabine-resistant AML cell lines (51,52), the mechanisms underlying cytarabine resistance remain unclear. The development of therapeutic resistance from this *in vitro* model is an important tool to understand the pathways underlying AML resistance acquisition.

Following the induction of cytarabine resistance, the present study verified that cytarabine treatment did not affect the HL-60R cell line *in vitro* and *in vivo*. Conversely, the parental cell line was demonstrated to be very sensitive to cytarabine treatment *in vitro*. The exposure of HL-60 cells to low doses of cytarabine was sufficient to decrease cell viability, increase Annexin V^+ cells and DNA fragmentation, and induce S phase arrest (data not shown). These effects are in agreement with previous studies describing the cytotoxic mechanisms underlying cytarabine treatment (53-55). Chen *et al* (56) demonstrated that mice injected subcutaneously with HL-60 cells exhibited a reduction in tumor size following cytarabine treatment. Since the HL-60 cell line demonstrated decreased capacity to generate tumors in xenograft models in comparison to the HL-60R cell line, the HL-60R cytarabine resistance phenotype was validated *in vitro* and *in vivo*. Taken together, the present results indicated that the HL-60R cell line may be

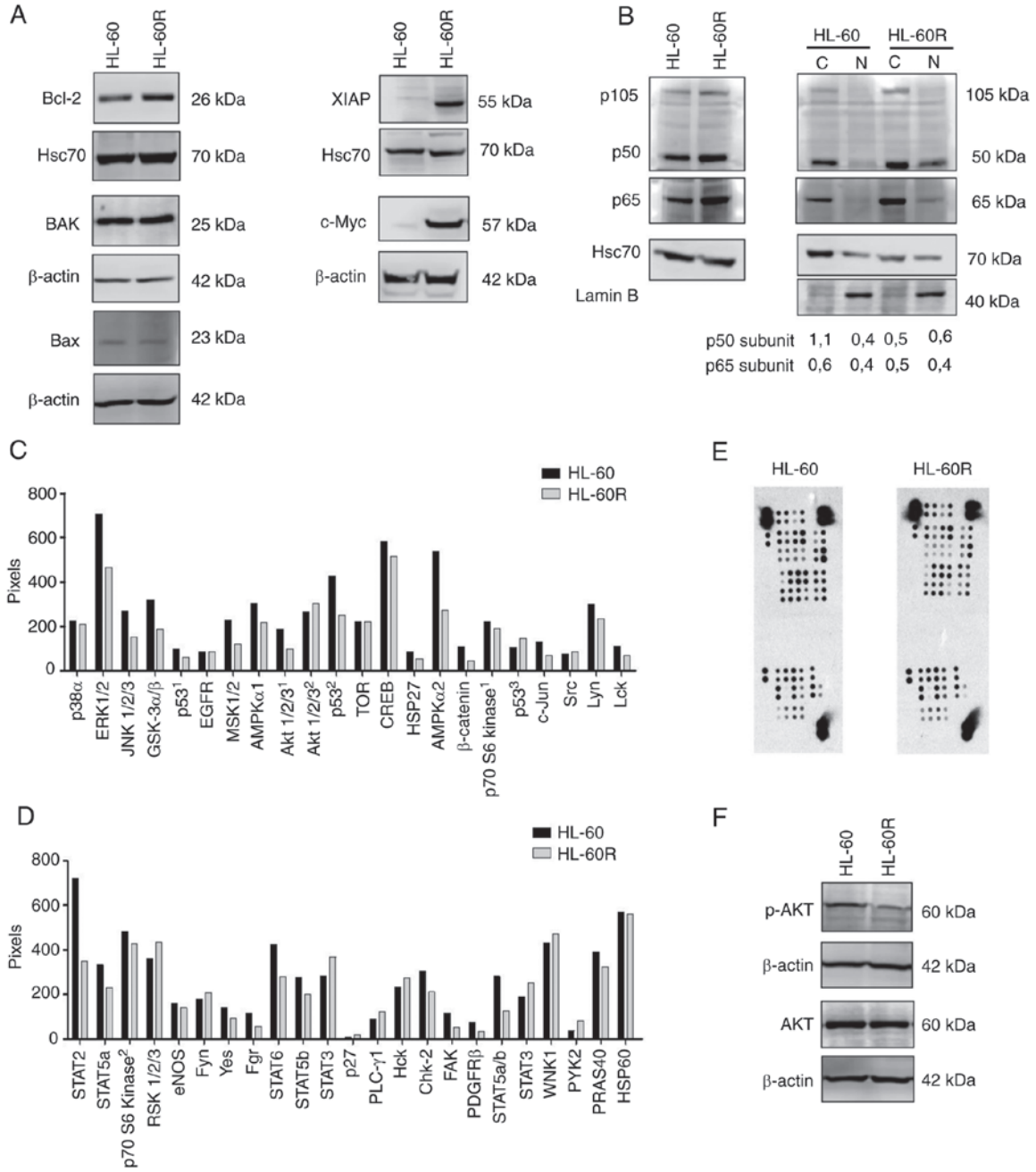

Figure 4. Induction of cytarabine resistance affects the protein phosphorylation pattern, and enhances the expression levels of anti-apoptotic proteins, c-Myc and nuclear NF-κB p50. (A) Protein expression of apoptotic and proliferative-related proteins in HL-60R and HL-60 cell lines. (B) p50 and p65 NF-κB protein expression and localization in HL-60 and HL-60R cell lines. (C and D) Quantification of protein phosphorylation levels detected in HL-60 and HL-60R cells by phospho-kinase array. (E) Representative images of the phospho-kinase array. (F) Protein expression levels of AKT 1/2/3 in HL-60 and HL-60R cells, to validate the phospho-kinase array. Representative images of three independent experiments are shown. XIAP, X-linked inhibitor of apoptosis protein; C, cytoplasmic fraction; N, nuclear fraction; p-AKT, phosphorylated-AKT.

considered an interesting model to study the specific pathways involved in acquisition of cytarabine resistance.

AML response to cytarabine depends on several factors, such as patient mutational profile, age, white-blood cell count and karyotype (1,3). Complex karyotypes in AML are associated with poor prognosis and treatment response (57-59). The HL-60 cell line presents two sub-populations with complex karyotypes co-existing in the same cell culture, whereas HL-60R presents a single sub-population, also with a complex aberrant karyotype. Notably, these cell lines do not harbor mutations highly associated with leukemia development, poor prognosis and low treatment response in AML, such as *CEBPα*, *ITD-FLT3*, *NPM1*, *c-KIT* and others (60-62). Thus, it may be hypothesized that chromosomal alterations could be a predominant genetic force underlying the lack of response to cytarabine treatment in HL-60R cells (58-63).

Resistance induction in HL-60R cells led to several molecular alterations that are intrinsically linked to the absence of response to cytarabine-induced apoptosis. Apoptosis evasion is a significant obstacle in chemotherapy response in several types of cancer, including AML (64,65). The results of the present study demonstrated that acquired cytarabine

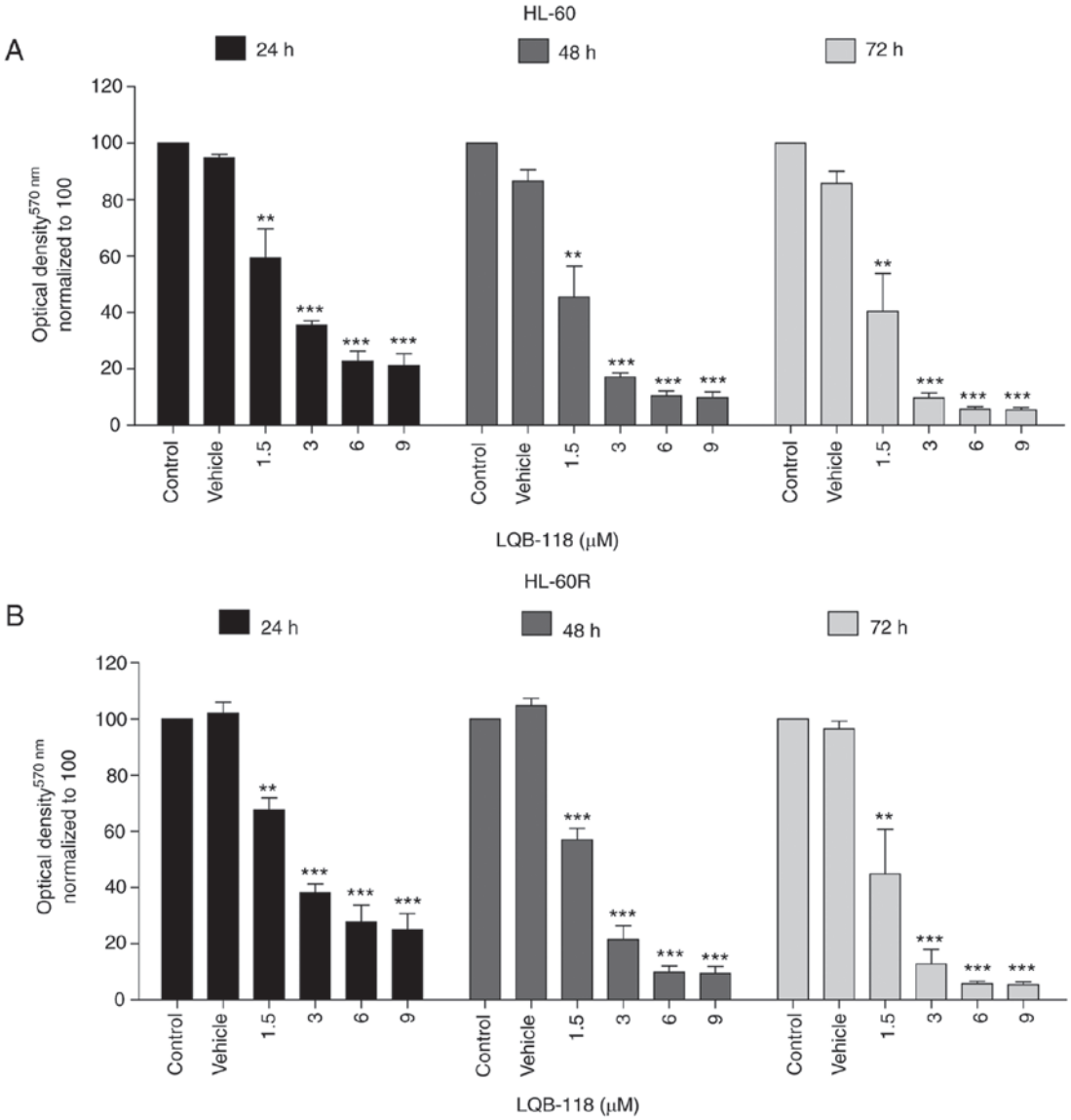

Figure 5. LQB-118 reduces the viability of cytarabine-resistant cells and parental cells. (A) HL-60 and (B) HL-60R cells were treated with 1.5-9 μM LQB-118 and cell viability was evaluated by MTT assay after 24, 48 and 72 h. Optical density was normalized to the control group, which was set at 100. Data are presented as the mean ± SD of three independent experiments. Statistical significance was determined by one-way ANOVA and Bonferroni post-hoc test. **P≤0.01, ***P≤0.001 vs. vehicle group.

resistance in HL-60R cells promoted the upregulation of the anti-apoptotic protein Bcl-2; however, no alterations were observed in the expression levels of the pro-apoptotic proteins BAK and Bax. Corroborating these data, high Bcl-2/Bax ratios were previously revealed to be associated with decreased rates of OS and complete remission in AML (18,65), which might be closely linked to the acquisition of cytarabine resistance.

IAP family members serve a significant role in conferring poor prognosis to patients with AML (66). Previous studies revealed that XIAP upregulation could be associated with AML poor prognosis (65-67), as well as with doxorubicin resistance *in vitro* and poor response to chemotherapy in the first 30 days of patient treatment (67,68). Consistently, XIAP inhibition has been reported to sensitize AML cells to TRAIL and chemotherapy (65-69). In addition, high co-expression of XIAP and survivin proteins has been correlated with poor OS in childhood *de novo* AML (66,67). Survivin expression had no association with acquired cytarabine resistance (data not shown), whereas XIAP upregulation could potentially have an important role, which remains to be explored. NF-κB constitutive expression and activation has been shown to be closely related to chemotherapy resistance and poor prognosis in patients with AML (70,71). The present study demonstrated that acquired cytarabine resistance in the HL-60R cell line resulted in high nuclear localization of p50 and p65 subunits. When activated, NF-κB binds to DNA, and leads to the transcription of its target genes, some of which are associated with apoptosis evasion, such as Bcl-2. A previous study demonstrated that NF-κB activation induced higher levels of Bcl-2 in prostate cancer, which was related to poor response to hormone therapy (72). Furthermore, high expression and activity of NF-κB and elevated levels of Bcl-2 have been reported to be associated with poor outcome and chemotherapy response in several tumor types (73-76).

High levels of c-Myc transcription factor in patients with AML have been shown to be correlated to low OS rate (77).

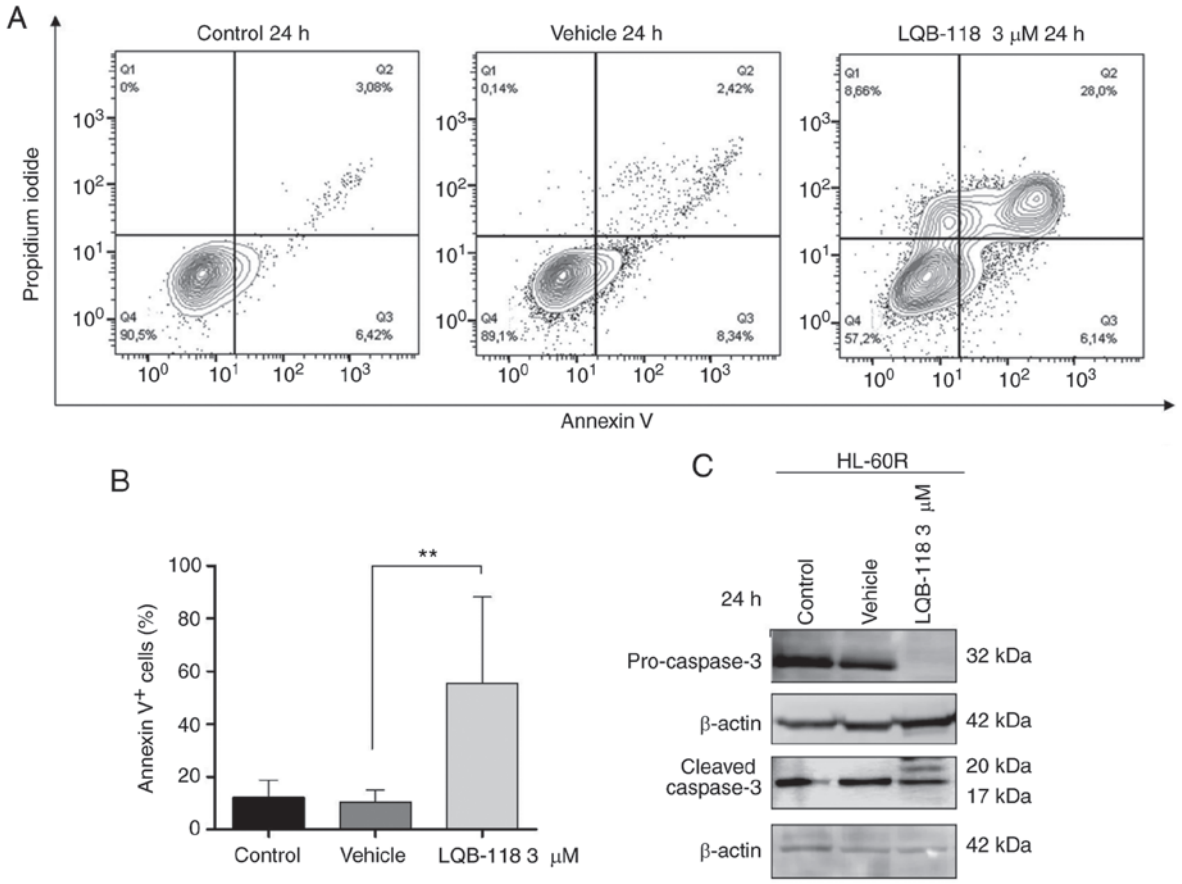

Figure 6. LQB-118 induces apoptosis of cytarabine-resistant cells. HL-60R cells were treated with LQB-118 (3 μM) for 24 h. (A and B) Treatment with LQB-118 enhanced the percentage of Annexin V$^+$ cells, as determined by flow cytometry, and (C) decreased pro-caspase-3 expression and induced caspase-3 cleavage. Representative image of three independent experiments are shown. Data are presented as the mean ± SD of three independent experiments. Statistical significance was determined by one-way ANOVA and Bonferroni post-hoc test. **P≤0.01.

Thus, the present study investigated the role of c-Myc in cytarabine-resistant AML cells; the results revealed that HL-60R cells presented high levels of c-Myc protein, but not c-Myc mRNA levels when compared with the parental cell line. In the model used in the present study, it is likely that elevated expression of c-Myc is not directly related to an increase of its transcription, and it might reflect an increase in c-Myc protein stability or regulation by post-translational modifications. It has already been demonstrated that the NF-κB p50 subunit can inhibit c-Myc degradation through FBW7 suppression (78). Since HL-60R cells present high levels of nuclear p50 and c-Myc protein expression, this could be a mechanism by which c-Myc degradation is inhibited, leading to the acquisition of cytarabine resistance. Furthermore, co-expression of c-Myc and Bcl-2 in aggressive B-cell lymphoma treated with cytarabine was revealed to be correlated to low OS and response to treatment induction (79). The present study also evaluated protein kinases, such as AKT, and demonstrated that several of these proteins were differentially phosphorylated in cytarabine-resistant cells compared with in cytarabine-sensitive cells. However, these findings require further investigation to improve understanding on the role of these kinases in cytarabine resistance.

Since cytarabine resistance remains an obstacle to AML treatment, the search for alternative treatment options to bypass acquired and intrinsic resistance is important. The LQB-118 compound is a pterocarpanquinone with antitumor effects toward diverse types of hematological and solid tumors *in vitro* and *in vivo* (25-29,40-43). However, to the best of our knowledge, no studies have assessed its antitumor activity in cytarabine-resistant established cells. Initially, the present study demonstrated that LQB-118 treatment decreased cell viability and induced apoptosis of HL-60R cells, but did not interfere with cell cycle progression. These data corroborated a previous study from our group, in which it was demonstrated that LQB-118 exerted an antitumor effect on the Kasumi-1 AML cell line and on patient samples with different molecular backgrounds (25). The Kasumi-1 cell line is an AML M2 sub-type with t(8;21), which is intrinsically resistant to cytarabine (80) and similarly responsive to LQB-118 treatment as HL-60R cells *in vitro*, suggesting that LQB-118 activity in resistant cell lines is independent of whether the resistance phenotype is acquired or intrinsic.

Previous studies have already demonstrated the significance of XIAP in AML cytarabine resistance (19,66-68). The present study revealed that the expression levels of the anti-apoptotic proteins XIAP and Bcl-2 were increased in the HL-60R cell line after cytarabine exposure, suggesting that these proteins may be involved in the acquisition of cytarabine resistance. Moreover, it was demonstrated that the protein expression levels of XIAP were reduced in response

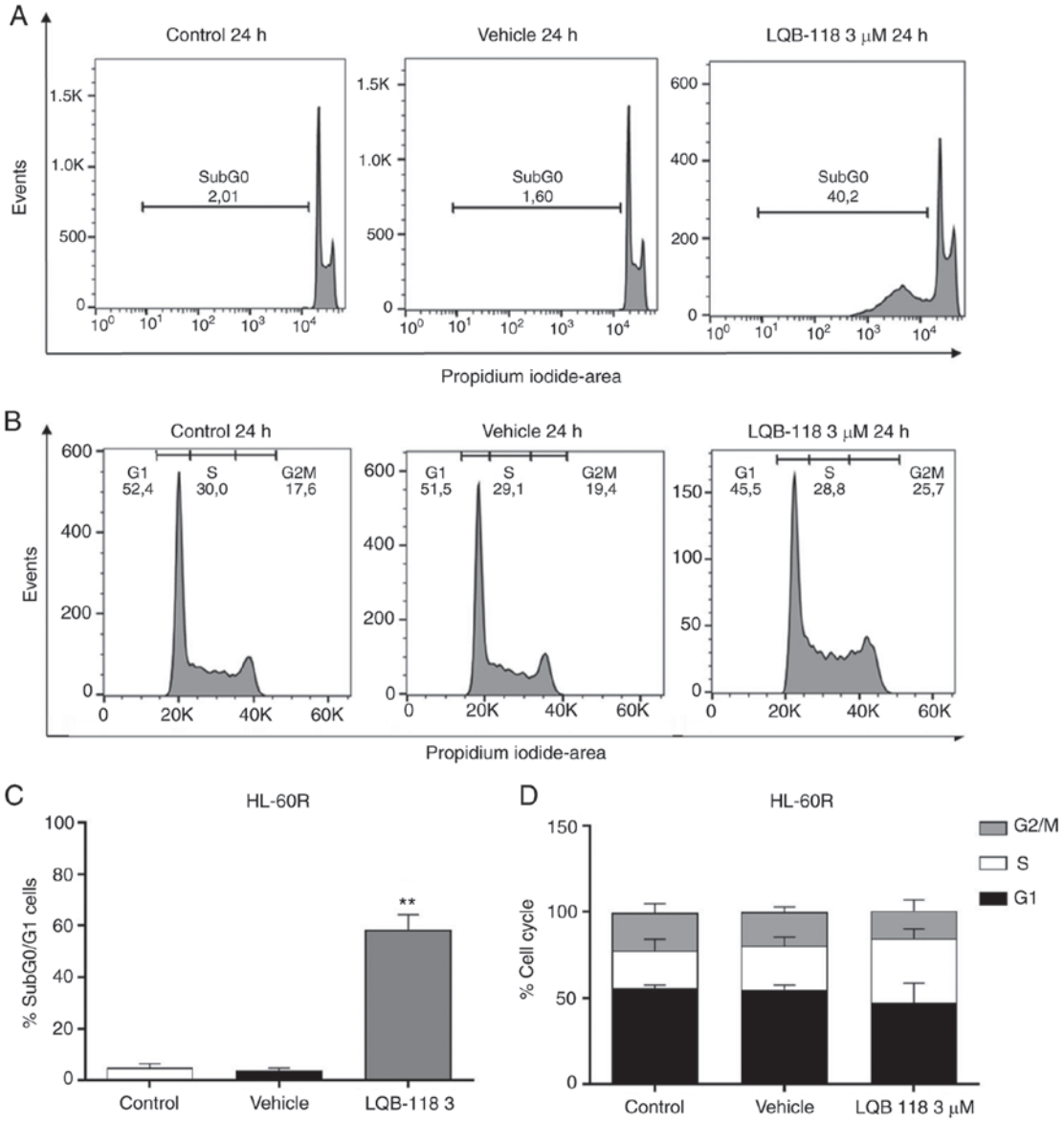

Figure 7. LQB-118 induces DNA fragmentation in HL-60R cells, but does not affect cell cycle profile. HL-60R cells were treated with 3 μM LQB-118 for 24 h. After treatment, (A and C) DNA fragmentation and (B and D) cell cycle progression were assessed by flow cytometry. Data are presented as the mean ± SD of three independent experiments. Statistical significance was determined by one-way ANOVA and Bonferroni post-hoc test. **P≤0.01 vs. vehicle group.

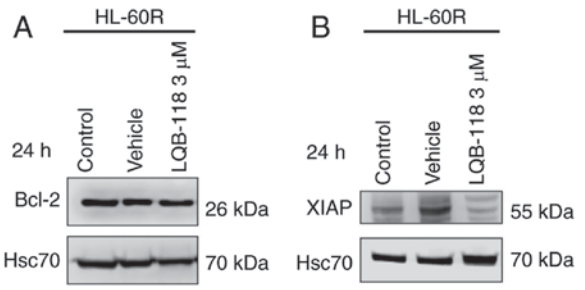

Figure 8. LQB-118 inhibits XIAP expression but does not affect Bcl-2 expression in cytarabine-resistant cells. Protein expression levels of (A) XIAP and (B) Bcl-2 were evaluated after HL-60R cells were treated with LQB-118 (3 μM) for 24 h. Representative image of three independent experiments are shown. XIAP, X-linked inhibitor of apoptosis protein.

to LQB-118 treatment in HL-60R cells *in vitro*, which is consistent with our previous findings in Kasumi-1 cells (25). In addition, it is well known that a feedback loop exists between XIAP and NF-κB activation (81,82), which might partially explain the reason why both proteins were upregulated in HL-60R cells. De Faria *et al* (41) observed that treatment with LQB-118 in CML cell lines induced modulation of NF-κB subcellular localization. Furthermore the same effect was also observed in the Kasumi-1 AML cell line treated with LQB-118 (25). Considering the present data and the results of previous studies, it may be hypothesized that LQB-118 induces apoptosis of cytarabine-resistant cells possibly through NF-κB modulation, which in turn may result in decreased XIAP expression.

In summary, the present data indicated that acquired cytarabine resistance in AML may be a multifactorial process, involving chromosomal aberrations and differential expression of signaling pathways associated with apoptosis and cell proliferation. Moreover, the present study suggested that LQB-118 might be a promising alternative therapeutic

approach for the treatment of patients with AML that are non-responsive to standard treatment.

Acknowledgements

Not applicable.

Funding

This work was supported by the Conselho Nacional de Desenvolvimento Científico e Tecnológico (CNPq; grant nos. 304565/2016-4 and 429687/2018-4) and the Fundação para Amparo à Pesquisa do Estado do Rio de Janeiro (FAPERJ; grant no. E26/202-798/2017).

Availability of data and materials

The datasets used and/or analyzed during the current study are available from the corresponding author on reasonable request.

Authors' contributions

TH designed the experiments, generated the cytarabine-resistant cell line, performed the viability and cellular effects assays (MTT, cell death, DNA fragmentation and cell cycle profile assays), and protein expression analysis, analyzed the data and wrote the manuscript. LM analyzed the flow cytometry experiments. GG performed and analyzed the *in vivo* assays. MR performed and analyzed the qPCR experiments. BDSM and GNEM performed analysis of expression and subcellular localization of NF-κB family members. BCRM and LMG performed the mutational screening experiments. LODC performed the karyotype analysis. PRRC and CDN synthesized the LQB-118 compound. FCCDF designed experiments, analyzed the data and revised the manuscript draft. RCM designed the study, provided all the resources and revised the manuscript draft. TH and RCM confirm the authenticity of all the raw data. All authors read and approved the final manuscript.

Ethics approval and consent to participate

All animal experiments were approved by the Animal Ethics Committees from INCA.

Patient consent for publication

Not applicable.

Competing interests

The authors declare that they have no competing interests.

References

1. Estey EH: Acute myeloid leukemia: 2014 update on risk-stratification and management. Am J Hematol 89: 1063-1081, 2014.
2. Saultz JN and Garzon R: Acute myeloid leukemia: A concise review. J Clin Med 5: 33, 2016.
3. De Kouchkovsky I and Abdul-Hay M: 'Acute myeloid leukemia: A comprehensive review and 2016 update'. Blood Cancer J 6, e441, 2016.
4. Burnett AK: Treatment of acute myeloid leukemia: Are we making progress? Hematology Am Soc Hematol Educ Program 2012: 1-6, 2012.
5. Sakamoto KM, Grant S, Saleiro D, Crispino JD, Hijiya N, Giles F, Platanias L and Eklund EA: Targeting novel signaling pathways for resistant acute myeloid leukemia. Mol Genet Metab 114: 397-402, 2015.
6. Feliciano SV, Santos MO, Pombo-de-Oliveira MS, de Aquino JA, de Aquino TA, Arregi MM, Antoniazzif BN, da Costa AM, Formigosa LA, Laporte CA, *et al*: Incidence and mortality of myeloid malignancies in children, adolescents and Young adults in Brazil: A population-based study. Cancer Epidemiol 62: 101583, 2019.
7. Schlenk RF and Döhner H: Genomic applications in the clinic: Use in treatment paradigm of acute myeloid leukemia. Hematology Am Soc Hematol Educ Program 2013: 324-330, 2013.
8. Yeung CC and Radich J: Predicting chemotherapy resistance in AML. Curr Hematol Malig Rep 12: 530-536, 2017.
9. Coombs CC, Tallman MS and Levine RL: Molecular therapy for acute myeloid leukaemia. Nat Rev Clin Oncol 13: 305-318, 2016.
10. Murphy T and Yee KW: Cytarabine and daunorubicin for the treatment of acute myeloid leukemia. Expert Opin Pharmacother 18: 1765-1780, 2017.
11. Rustum YM and Preisler HD: Correlation between leukemic cell retention of 1-beta-D-arabinofuranosylcytosine 5'-triphosphate and response to therapy. Cancer Res 39: 42-49, 1979.
12. Löwenberg B, Pabst T, Vellenga E, van Putten W, Schouten HC, Graux C, Ferrant A, Sonneveld P, Biemond BJ, Gratwohl A, *et al*: Cytarabine dose for acute myeloid leukemia. N Engl J Med 364: 1027-1036, 2011.
13. Rowe JM: AML in 2017: Advances in clinical practice. Best Pract Res Clin Haematol 30: 283-286, 2017.
14. Kayser S and Levis MJ: Advances in targeted therapy for acute myeloid leukaemia. Br J Haematol 180: 484-500, 2018.
15. Negoro E, Yamauchi T, Urasaki Y, Nishi R, Hori H and Ueda T: Characterization of cytarabine-resistant leukemic cell lines established from five different blood cell lineages using gene expression and proteomic analyses. Int J Oncol 38: 911-919, 2011.
16. Tamm I, Richter S, Oltersdorf D, Creutzig U, Harbott J, Scholz F, Karawajew L, Ludwig WD and Wuchter C: High expression levels of x-linked inhibitor of apoptosis protein and survivin correlate with poor overall survival in childhood de novo acute myeloid leukemia. Clin Cancer Res 10: 3737-3744, 2004.
17. Chromik J, Safferthal C, Serve H and Fulda S: Smac mimetic primes apoptosis-resistant acute myeloid leukaemia cells for cytarabine-induced cell death by triggering necroptosis. Cancer Lett 344: 101-109, 2014.
18. Kulsoom B, Shamsi TS, Afsar NA, Memon Z, Ahmed N and Hasnain SN: Bax, Bcl-2, and Bax/Bcl-2 as prognostic markers in acute myeloid leukemia: Are we ready for Bcl-2-directed therapy? Cancer Manag Res 10: 403-416, 2018.
19. Shang J, Chen WM, Wang ZH, Wei TN, Chen ZZ and Wu WB: CircPAN3 mediates drug resistance in acute myeloid leukemia through the miR-153-5p/miR-183-5p-XIAP axis. Exp Hematol 70: 42-54.e3, 2019.
20. Kaltschmidt B, Greiner JFW, Kadhim HM and Kaltschmidt C: Subunit-specific role of NF-κB in cancer. Biomedicines 6: 44, 2018.
21. Colombo F, Zambrano S and Agresti A: NF-kappaB, the importance of being dynamic: Role and insights in cancer. Biomedicines 6: 45, 2018.
22. Guzman ML, Neering SJ, Upchurch D, Grimes B, Howard DS, Rizzieri DA, Luger SM and Jordan CT: Nuclear factor-kappaB is constitutively activated in primitive human acute myelogenous leukemia cells. Blood 98: 2301-2307, 2001.
23. Xia B, Tian C, Guo S, Zhang L, Zhao D, Qu F, Zhao W, Wang Y, Wu X, Da W, *et al*: c-Myc plays part in drug resistance mediated by bone marrow stromal cells in acute myeloid leukemia. Leuk Res 39: 92-99, 2015.
24. Mughal MK, Akhter A, Street L, Pournazari P, Shabani-Rad MT and Mansoor A: Acute myeloid leukaemia: Expression of MYC protein and its association with cytogenetic risk profile and overall survival. Hematol Oncol 35: 350-356, 2017.
25. de Souza Reis FR, de Faria FC, Castro CP, de Souza PS, da Cunha Vasconcelos F, Bello RD, da Silva AJ, Costa PR and Maia RC: The therapeutical potential of a novel pterocarpanquinone LQB-118 to target inhibitor of apoptosis proteins in acute myeloid leukemia cells. Anticancer Agents Med Chem 13: 341-351, 2013.

26. Nestal De Moraes G, Pereira Castro C, Salustiano EJ, Dumas ML, Costas F, Wing-Fai Lam E, Ribeiro Costa PR and Maia RC: [Corrigendum] The pterocarpanquinone LQB-118 induces apoptosis in acute myeloid leukemia cells of distinct molecular subtypes and targets FoxO3a and FoxM1 transcription factors. Int J Oncol 55: 1396, 2019.
27. Maia RC, Vasconcelos FC, de Sá Bacelar T, Salustiano EJ, da Silva LF, Pereira DL, Moellman-Coelho A, Netto CD, da Silva AJ, Rumjanek VM and Costa PR: LQB-118, a pterocarpanquinone structurally related to lapachol [2-hydroxy-3-(3-methyl-2-butenyl)-1,4-naphthoquinone]: A novel class of agent with high apoptotic effect in chronic myeloid leukemia cells. Invest New Drugs 29: 1143-1155, 2011.
28. de Sa Bacelar T, da Silva AJ, Costa PR and Rumjanek VM: The pterocarpanquinone LQB 118 induces apoptosis in tumor cells through the intrinsic pathway and the endoplasmic reticulum stress pathway. Anticancer Drugs 24: 73-83, 2013.
29. Netto CD, da Silva AJ, Salustiano EJ, Bacelar TS, Rica IG, Cavalcante MC, Rumjanek VM and Costa PR: New pterocarpanquinones: Synthesis, antineoplasic activity on cultured human malignant cell lines and TNF-alpha modulation in human PBMC cells. Bioorg Med Chem 18: 1610-1616, 2010.
30. McGowan-Jordan J, Simons A and Schmid M: ISCN 2016. In: An International System for Human Cytogenomic Nomenclature (2016). Karger AG, Basel, 2016.
31. Livak KJ and Schmittgen TD: Analysis of relative gene expression data using real-time quantitative PCR and the 2(-Delta Delta C(T)) method. Methods 25: 402-408, 2001.
32. Faustino-Rocha A, Oliveira PA, Pinho-Oliveira J, Teixeira-Guedes C, Soares-Maia R, da Costa RG, Colaco B, Pires MJ, Colaco J, Ferreira R and Ginja M: Estimation of rat mammary tumor volume using caliper and ultrasonography measurements. Lab Anim (NY) 42: 217-224, 2013.
33. Tomayko MM and Reynolds CP: Determination of subcutaneous tumor size in athymic (nude) mice. Cancer Chemother Pharmacol 24: 148-154, 1989.
34. Yang Y, Xue K, Li Z, Zheng W, Dong W, Song J, Sun S, Ma T and Li W: [Corrigendum] cMyc regulates the CDK1/cyclin B1 dependentG2/M cell cycle progression by histone H4 acetylation in Raji cells. Int J Mol Med 44: 1988, 2019.
35. Zuber J, Radtke I, Pardee TS, Zhao Z, Rappaport AR, Luo W, McCurrach ME, Yang MM, Dolan ME, Kogan SC, *et al*: Mouse models of human AML accurately predict chemotherapy response. Genes Dev 23: 877-889, 2009.
36. Liersch R, Muller-Tidow C, Berdel WE and Krug U: Prognostic factors for acute myeloid leukaemia in adults-biological significance and clinical use. Br J Haematol 165: 17-38, 2014.
37. Lynch RC and Medeiros BC: Chemotherapy options for previously untreated acute myeloid leukemia. Expert Opini Pharmacother 16: 2149-2162, 2015.
38. Carroll PA, Freie BW, Mathsyaraja H and Eisenman RN: The MYC transcription factor network: Balancing metabolism, proliferation and oncogenesis. Front Med 12: 412-425, 2018.
39. Park S, Chapuis N, Tamburini J, Bardet V, Cornillet-Lefebvre P, Willems L, Green A, Mayeux P, Lacombe C and Bouscary D: Role of the PI3K/AKT and mTOR signaling pathways in acute myeloid leukemia. Haematologica 95: 819-828, 2010.
40. Martino T, Magalhaes FC, Justo GA, Coelho MG, Netto CD, Costa PR and Sabino KC: The pterocarpanquinone LQB-118 inhibits tumor cell proliferation by downregulation of c-Myc and cyclins D1 and B1 mRNA and upregulation of p21 cell cycle inhibitor expression. Bioorg Med Chem 22: 3115-3122, 2014.
41. de Faria FC, Leal ME, Bernardo PS, Costa PR and Maia RC: NFκB pathway and microRNA-9 and -21 are involved in sensitivity to the pterocarpanquinone LQB-118 in different CML cell lines. Anticancer Agents Med Chem 15: 345-352, 2015.
42. Martino T, Kudrolli TA, Kumar B, Salviano I, Mencalha A, Coelho MG, Justo G, Costa PR, Sabino KC and Lupold SE: The orally active pterocarpanquinone LQB-118 exhibits cytotoxicity in prostate cancer cell and tumor models through cellular redox stress. Prostate 78: 140-151, 2018.
43. Bernardo PS, Guimaraes GH, De Faria FC, Longo G, Lopes GP, Netto CD, Costa PR and Maia RC: LQB118 compound inhibits migration and induces cell death in glioblastoma cells. Oncol Rep 43: 346-357, 2020.
44. Veisani Y, Khazaei S and Delpisheh A: 5-year survival rates based on the type of leukemia in Iran, a meta-analysis. Caspian J Intern Med 9: 316-324, 2018.
45. Lagunas-Rangel FA, Chavez-Valencia V, Gomez-Guijosa MA and Cortes-Penagos C: Acute myeloid leukemia-genetic alterations and their clinical prognosis. Int J Hematol Oncol Stem Cell Res 11: 328-339, 2017.
46. Hackl H, Astanina K and Wieser R: Molecular and genetic alterations associated with therapy resistance and relapse of acute myeloid leukemia. J Hematol Oncol 10: 51, 2017.
47. Walter RB, Othus M, Burnett AK, Lowenberg B, Kantarjian HM, Ossenkoppele GJ, Hills RK, Ravandi F, Pabst T, Evans A, *et al*: Resistance prediction in AML: Analysis of 4601 patients from MRC/NCRI, HOVON/SAKK, SWOG and MD anderson cancer center. Leukemia 29: 312-320, 2015.
48. Gallagher R, Collins S, Trujillo J, McCredie K, Ahearn M, Tsai S, Metzgar R, Aulakh G, Ting R, Ruscetti F and Gallo R: Characterization of the continuous, differentiating myeloid cell line (HL-60) from a patient with acute promyelocytic leukemia. Blood 54: 713-33, 1979.
49. Dalton WT Jr, Ahearn MJ, McCredie KB, Freireich, EJ, Stass SA and Trujillo JM: HL-60 cell line was derived from a patient with FAB-M2 and not FAB-M3. Blood 71: 242-247, 1988.
50. Collins SJ: The HL-60 promyelocytic leukemia cell line: Proliferation, differentiation, and cellular oncogene expression. Blood 70: 1233-1244, 1987.
51. Yamauchi T, Uzui K, Nishi R, Shigemi H and Ueda T: Cytarabine-resistant leukemia cells are moderately sensitive to clofarabine in vitro. Anticancer Res 34: 1657-1662, 2014.
52. Prenkert M, Uggla B, Tidefelt U and Strid H: CRIM1 is expressed at higher levels in drug-resistant than in drug-sensitive myeloid leukemia HL60 cells. Anticancer Res 30: 4157-4161, 2010.
53. Furth JJ and Cohen SS: Inhibition of mammalian DNA polymerase by the 5'-triphosphate of 1-beta-d-arabinofuranosylcytosine and the 5'-triphosphate of 9-beta-d-arabinofuranoxyladenine. Cancer Res 28: 2061-2067, 1968.
54. Kufe DW, Major PP, Egan EM and Beardsley GP: Correlation of cytotoxicity with incorporation of ara-C into DNA. J Biol Chem 255: 8997-8900, 1980.
55. Shepshelovich D, Edel Y, Goldvaser H, Dujovny T, Wolach O and Raanani P: Pharmacodynamics of cytarabine induced leucopenia: A retrospective cohort study. Br J Clin Pharmacol 79: 685-691, 2015.
56. Chen Y, Gan D, Huang Q, Luo X, Lin D and Hu J: Emodin and its combination with cytarabine induce apoptosis in resistant acute myeloid leukemia cells in vitro and in vivo. Cell Physiol Biochem 48: 2061-2073, 2018.
57. Slovak ML, Kopecky KJ, Cassileth PA, Harrington DH, Theil KS, Mohamed A, Paietta E, Willman CL, Head DR, Rowe JM, *et al*: Karyotypic analysis predicts outcome of preremission and postremission therapy in adult acute myeloid leukemia: A Southwest Oncology Group/Eastern Cooperative Oncology Group Study. Blood 96: 4075-4083, 2000.
58. Mrozek K: Cytogenetic, molecular genetic, and clinical characteristics of acute myeloid leukemia with a complex karyotype. Semin Oncol 35: 365-377, 2008.
59. Stölzel F, Mohr B, Kramer M, Oelschlagel U, Bochtler T, Berdel WE, Kaufmann M, Baldus CD, Schafer-Eckart K, Stuhlmann R, *et al*: Karyotype complexity and prognosis in acute myeloid leukemia. Blood Cancer J 6: e386, 2016.
60. Dash A and Gilliland DG: Molecular genetics of acute myeloid leukaemia. Best Pract Res Clin Haematol 14: 49-64, 2001.
61. Rubnitz JE, Gibson B and Smith FO: Acute myeloid leukemia. Hematol Oncol Clin North Am 24: 35-63, 2010.
62. Grove CS and Vassiliou GS: Acute myeloid leukaemia: A paradigm for the clonal evolution of cancer? Dis Model Mech 7: 941-951, 2014.
63. Kern W, Haferlach T, Schnittger S, Ludwig WD, Hiddemann W and Schoch C: Karyotype instability between diagnosis and relapse in 117 patients with acute myeloid leukemia: Implications for resistance against therapy. Leukemia 16: 2084-2091, 2002.
64. Cassier PA, Castets M, Belhabri A and Vey N: Targeting apoptosis in acute myeloid leukaemia. Br J Cancer 117: 1089-1098, 2017.
65. Del Poeta G, Bruno A, Del Principe MI, Venditti A, Maurillo L, Buccisano F, Stasi R, Neri B, Luciano F, Siniscalchi A, *et al*: Deregulation of the mitochondrial apoptotic machinery and development of molecular targeted drugs in acute myeloid leukemia. Curr Cancer Drug Targets 8: 207-222, 2008.
66. Tamm I, Kornblau SM, Segall H, Krajewski S, Welsh K, Kitada S, Scudiero DA, Tudor G, Qui YH, Monks A, *et al*: Expression and prognostic significance of IAP-family genes in human cancers and myeloid leukemias. Clin Cancer Res 6: 1796-1803, 2000.

67. Sung KW, Choi J, Hwang YK, Lee SJ, Kim HJ, Kim JY, Cho EJ, Yoo KH and Koo HH: Overexpression of X-linked inhibitor of apoptosis protein (XIAP) is an independent unfavorable prognostic factor in childhood de novo acute myeloid leukemia. J Korean Med Sci 24: 605-613, 2009.
68. Ibrahim AM, Mansour IM, Wilson MM, Mokhtar DA, Helal AM and Al Wakeel HM: Study of survivin and X-linked inhibitor of apoptosis protein (XIAP) genes in acute myeloid leukemia (AML). Lab Hematol 18: 1-10, 2012.
69. Zhou J, Lu X, Tan TZ and Chng WJ: X-linked inhibitor of apoptosis inhibition sensitizes acute myeloid leukemia cell response to TRAIL and chemotherapy through potentiated induction of proapoptotic machinery. Mol Oncol 12: 33-47, 2018.
70. Bosman MC, Schuringa JJ and Vellenga E: Constitutive NF-κB activation in AML: Causes and treatment strategies. Crit Rev Oncol Hematol 98: 35-44, 2016.
71. Rushworth SA, Zaitseva L, Murray MY, Shah NM, Bowles KM and MacEwan DJ: The high Nrf2 expression in human acute myeloid leukemia is driven by NF-κB and underlies its chemo-resistance. Blood 120: 5188-5198, 2012.
72. Catz SD and Johnson JL: Transcriptional regulation of bcl-2 by nuclear factor kappa B and its significance in prostate cancer. Oncogene 20: 7342-7351, 2001.
73. Murray S, Briasoulis E, Linardou H, Bafaloukos D and Papadimitriou C: Taxane resistance in breast cancer: Mechanisms, predictive biomarkers and circumvention strategies. Cancer Treat Rev 38: 890-903, 2012.
74. Alam M, Kashyap T, Pramanik KK, Singh AK, Nagini S and Mishra R: The elevated activation of NFκB and AP-1 is correlated with differential regulation of Bcl-2 and associated with oral squamous cell carcinoma progression and resistance. Clin Oral Investig 21: 2721-2731, 2017.
75. Xia Y, Shen S and Verma IM: NF-κB, an active player in human cancers. Cancer Immunol Res 2: 823-830, 2014.
76. Godwin P, Baird AM, Heavey S, Barr MP, O'Byrne KJ and Gately K: Targeting nuclear factor-kappa B to overcome resistance to chemotherapy. Front Oncol 3: 120, 2013.
77. Ohanian M, Rozovski U, Kanagal-Shamanna R, Abruzzo LV, Loghavi S, Kadia T, Futreal A, Bhalla K, Zuo Z, Huh YO, *et al*: MYC protein expression is an important prognostic factor in acute myeloid leukemia. Leuk Lymphoma 60: 37-48, 2019.
78. Huang H, Ma L, Li J, Yu Y, Zhang D, Wei J, Jin H, Xu D, Gao J and Huang C: NF-κB1 inhibits c-Myc protein degradation through suppression of FBW7 expression. Oncotarget 5: 493-505, 2014.
79. Miura K, Takahashi H, Nakagawa M, Izu A, Sugitani M, Kurita D, Sakagami M, Ohtake S, Uchino Y, Hojo A, *et al*: Clinical significance of co-expression of MYC and BCL2 protein in aggressive B-cell lymphomas treated with a second line immunochemotherapy. Leuk Lymphoma 57: 1335-1341, 2016.
80. Kobune M, Takimoto R, Murase K, Iyama S, Sato T, Kikuchi S, Kawano Y, Miyanishi K, Sato Y, Niitsu Y and Kato J: Drug resistance is dramatically restored by hedgehog inhibitors in $CD34^+$ leukemic cells. Cancer Sci 100: 948-955, 2009.
81. Lu M, Lin SC, Huang Y, Kang YJ, Rich R, Lo YC, Myszka D, Han J and Wu H: XIAP induces NF-kappaB activation via the BIR1/TAB1 interaction and BIR1 dimerization. Mol Cell 26: 689-702, 2007.
82. Hofer-Warbinek R, Schmid JA, Stehlik C, Binder BR, Lipp J and de Martin R: Activation of NF-kappa B by XIAP, the X chromosome-linked inhibitor of apoptosis, in endothelial cells involves TAK1. J Biol Chem 275: 22064-22068, 2000.